Journal of Experimental Nanoscience
Publication details, including instructions for authors and subscription information:
http://www.informaworld.com/smpp/title~content=t716100757

Synthesis of LaF_3: Yb^{3+} ,Ln^{3+} nanoparticles with improved upconversion luminescence

Huaxiang Shen[a]; Feng Wang[a]; Xianping Fan[a]; Minquan Wang[a]
[a] Department of Materials Science and Engineering, Zhejiang University, Hangzhou, P.R. China

To cite this Article Shen, Huaxiang , Wang, Feng , Fan, Xianping and Wang, Minquan(2007) 'Synthesis of LaF_3: Yb^{3+} ,Ln^{3+} nanoparticles with improved upconversion luminescence', Journal of Experimental Nanoscience, 2: 4, 303 — 311
To link to this Article: DOI: 10.1080/17458080701724943
URL: http://dx.doi.org/10.1080/17458080701724943

Journal of Experimental Nanoscience,
Vol. 2, No. 4, December 2007, 303–311

Taylor & Francis
Taylor & Francis Group

Synthesis of LaF_3: Yb^{3+},Ln^{3+} nanoparticles with improved upconversion luminescence

HUAXIANG SHEN, FENG WANG, XIANPING FAN*
and MINQUAN WANG

Department of Materials Science and Engineering, Zhejiang University,
Hangzhou 310027, P.R. China

(*Received March 2007; in final form September 2007*)

Yb^{3+}/Er^{3+} and Yb^{3+}/Tm^{3+} co-doped LaF_3 nanoparticles with upconversion luminescence properties were prepared via the co-precipitation method, followed by heat treatment at different temperatures in the range of 180°C to 600°C. We investigated the influence of heat treatment temperatures on the size, morphology, and upconversion luminescence intensity of the nanoparticles. Significant increases of the particle size and upconversion luminescence intensity of the nanoparticles were observed with increasing heat treatment temperature. The upconversion mechanism of the LaF_3:Yb^{3+},Er^{3+} and LaF_3:Yb^{3+},Tm^{3+} nanoparticles was also discussed.

Keywords: Lanthanide; Nanoparticles; Upconversion

1. Introduction

In the field of luminescent bio-labeling, considering their attractive optical and chemical features such as low toxicity, large effective Stokes shifts, as well as high resistance to photobleaching, blinking, and photochemical degradation, lanthanide-doped luminescent nanoparticles were proposed to be a promising new class of luminescent labelling agents, which have the potential and ability to overcome a number of problems associated with the commonly used luminescent labels [1–3]. In particular, lanthanide-doped luminescent materials have the unique feature of converting near infrared photons (NIR) to visible (VIS) in a process known as upconversion [4, 5]. Labelling with lanthanide-doped upconversion nanoparticles can circumvent auto-fluorescence from and photo-damage to the biological specimens associated with conventional luminescent labelling technologies [6, 7], which are mostly based on the use of ultraviolet (UV) or short wavelength visible (VIS) irradiation.

*Corresponding author. Email: fanxp@cmsce.zju.edu.cn

Journal of Experimental Nanoscience
ISSN 1745–8080 print/ISSN 1745–8099 online © 2007 Taylor & Francis
http://www.tandf.co.uk/journals
DOI: 10.1080/17458080701724943

The concept of using NIR irradiation to generate VIS emission for bio-applications first appeared in 1990, through a multi-photon microscopy technique [8]. However, in multi-photon excitation processes, a high photon flux at $MW\,cm^{-1}$ and $GW\,cm^{-1}$ intensities needs to be delivered to the sample because multi-photon absorption involves a non-stationary quantum mechanical state and thus exhibits very low efficiency [9]. To avoid thermal decomposition processes in the sample, expensive ultrashort pulsed lasers are frequently employed as light sources. In comparison, lanthanide-doped upconversion nanoparticles are more preferable since they can easily be excited by economical continuous wave (cw) diode laser source at conventional excitation light intensities, as a result of the ladder-like arranged electronic states of the trivalent lanthanide ions [4, 5].

The preparation of lanthanide-doped upconversion nanoparticles has been reported previously. However, in the beginning the host matrices involved were mostly oxides [10–13]. Very high temperatures were required to prepare these materials and thus the products usually show low process ability. In addition, oxides usually have high vibrational energies, which would cause significant loss of the excitation energy of the luminescent center and thus lead to low upconversion efficiency. Therefore, oxide nanoparticles were not the optimal candidates for using as upconversion biolabels. In recent years, fluoride nanoparticles have attracted increasing attention due to their low vibrational energies and ease of preparation. The syntheses of lanthanide-doped $NaYF_4$, $NaGdF_4$, GdF_3, YF_3, and LaF_3 nanoparticles that can disperse in various solvents and exhibit strong upconversion luminescence have also been reported [14–23].

LaF_3 is a typical fluoride characterized by its adequate thermal and environmental stability as well as large solubility for all lanthanide ions [24, 25]. Therefore, LaF_3 is one of the most frequently used host materials for luminescent lanthanide ions. So far, lanthanide-doped LaF_3 nanoparticles have been extensively studied [26–29]. LaF_3 nanoparticles with upconversion luminescence properties have also been reported before [20, 23]. However, most of the previous studies only aimed at the development of a new synthesis method to prepare LaF_3 nanoparticles with controlled size and tailored surface property. Little attention has been paid to the enhancement of upconversion luminescence, which is also crucial to their practical applications. In this paper, we prepared Yb^{3+}/Er^{3+} and Yb^{3+}/Tm^{3+} co-doped LaF_3 nanoparticles by a very simple co-precipitation method. Aiming at enhancing the upconversion luminescence, we then annealed the samples at different temperatures and investigated the effect of heat treatment temperatures on the size, morphology, and upconversion luminescence intensity of the nanoparticles. We also studied the upconversion mechanism of the LaF_3:Yb^{3+},Er^{3+} and LaF_3:Yb^{3+},Tm^{3+} nanoparticles.

2. Experimental

In a typical procedure to prepare the lanthanide-doped LaF_3 nanoparticles, 0.4 mmol $LnCl_3$ (Ln = La, Yb, Er/Tm) were added to a beaker containing 100 ml ethanol. After being stirred magnetically for about 10 min, the mixture became a colorless transparent solution. Then, slightly excessive ammonium fluoride (1.5 mmol NH_4F)

was added to the beaker. After being stirred for 4 h at 60°C, the precipitated powders were separated by centrifugation, washed with deionized water and ethanol for several times, and then dried in an oven at 50°C for 12 h. To study the effects of heat treatment on the properties of the products, the as-prepared nanoparticles were annealed for 2 h at different temperature (180°C, 400°C, and 600°C) in a stove and collected for characterisation.

The phase and crystal structure were analysed by X-ray diffraction (XRD) (Philips XD98) using Cu Kα radiation. Transmission electron microscope (TEM) images were taken on a JEM-1230 microscope operating at 80 kV. The upconversion emission spectra were taken on the Hitachi F-4500 fluorescence spectrophotometer with an external 980-nm LD as the excitation source, instead of the xenon source in the spectrophotometer. Differential thermal analysis (DTA) and thermal gravity (TG) measurements were carried out in a CDR-1 differential thermal analyser in order to detect the other effects of heat treatment on the as-prepared LaF_3 nanoparticles.

3. Results and discussion

Figure 1 shows the transmission electron microscope (TEM) images of the 20 mol% Yb^{3+} and 2 mol% Er^{3+} co-doped nanoparticles as prepared and after heat treatment for 2 h at different temperatures. The size of the nanoparticles increased rapidly from less than 10 nm to around 100 nm with elevating heat treatment temperatures, indicating growth of the nanoparticles happened during the heat treatment processes. Due to reduction in the surface energy caused by increase of the particle size, less agglomeration was observed for samples annealing at higher temperatures.

The crystal phase of the nanoparticles was determined by X-ray powder diffraction. Figure 2(a) gives XRD patterns of the 20 mol% Yb^{3+} and 2 mol% Er^{3+} co-doped nanoparticles synthesized at different temperatures. Compared to the JCPDS standard card (32-0483) of the hexagonal LaF_3 crystal, there were no excessive peaks, indicating the formation of the single-phase hexagonal crystalline of LaF_3. From figure 2(a) we can also observe that with increasing heat treatment temperature the intensity of the diffraction peaks increase gradually and the full width at half maximum (FWHM) of the peaks reduced gradually, indicating improvement of the particle crystallinity and increase of the particle size. The mean particle size of the nanoparticle can be estimated roughly from the broadening of the peaks by using the Scherrer formula. Figure 2(b) shows the relationship between the heat treatment temperatures and particle diameters determined by fitting (111) diffraction peak to Scherrer formula. As can be seen, the particle size increased only slightly at heat treatment temperatures below 400°C. Heat treatment above this temperature will cause significant increase of the particle size over 100 nm. Thus, a heat treatment temperature of lower than 400°C is suitable for preparing LaF_3 nanoparticles.

To investigate other effects of the heat treatment, the DTA-TG analysis of the as prepared 20 mol% Yb^{3+} and 2 mol% Er^{3+} co-doped nanoparticles was taken and the results are given in figure 3. The TG diagram exhibits two obvious weight-losses in the temperature ranges of 70–90°C and 90–250°C. The weight–loss in the temperature

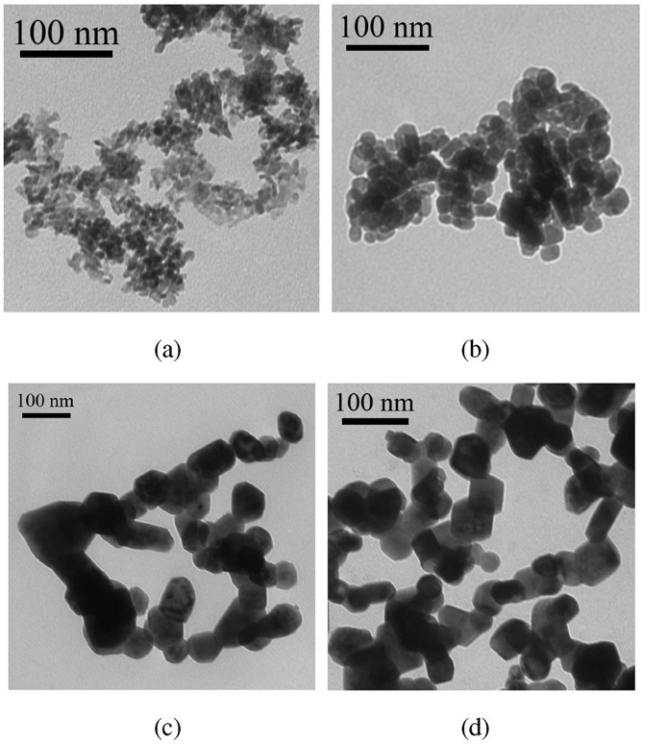

Figure 1. TEM images of 20 mol% Yb^{3+} and 2 mol% Er^{3+} co-doped LaF_3 nanoparticles (a) as-prepared and after heat treatment at (b) 180°C, (c) 400°C, and (d) 600°C.

range of 70–90°C can be attributed to the evaporation of the ethanol molecules, and the weight-loss in the temperature range of 90–250°C was due to the removal of the OH^- groups, NH_4Cl, and NH_4F from the particle surface, respectively. In the DTA diagram, two endothermic peaks at about 90°C and 200°C can be observed, which correspond to the weight losses mentioned above. In addition, broad exothermic peaks starting at about 500°C were also observed in the DTA diagram, which can be attributed to the crystal structure adjustments of the nanoparticles.

The upconversion spectra of the 20 mol% Yb^{3+} and 2 mol% Er^{3+} co-doped nanoparticles synthesized at different temperatures are depicted in figure 4. The emission spectrum exhibits typical Er^{3+} emission peaks at the 411 nm, 525 nm, 539 nm, and 653 nm, which can be assigned to $^4H_{9/2} \rightarrow {}^4I_{15/2}$, $^4H_{11/2} \rightarrow {}^4I_{15/2}$, $^4S_{3/2} \rightarrow {}^4I_{15/2}$, and $^4F_{9/2} \rightarrow {}^4I_{15/2}$ transitions, respectively. It can also be observed from the upconversion spectra that the intensities of upconversion luminescence increase rapidly with increase of the heat treatment temperatures. The upconversion emissions of nanoparticles that were heat treated at above 400°C were so strong that they are visible to naked eyes when excited with a laser diode of about 50 mW at 980 nm. When samples were heat treated at high temperatures, the crystal structure of host materials can be improved and thus the solubility of lanthanide ions can be raised, which resulted in part elimination of the ion cluster [30] and thus reduced the loss of excited energy by

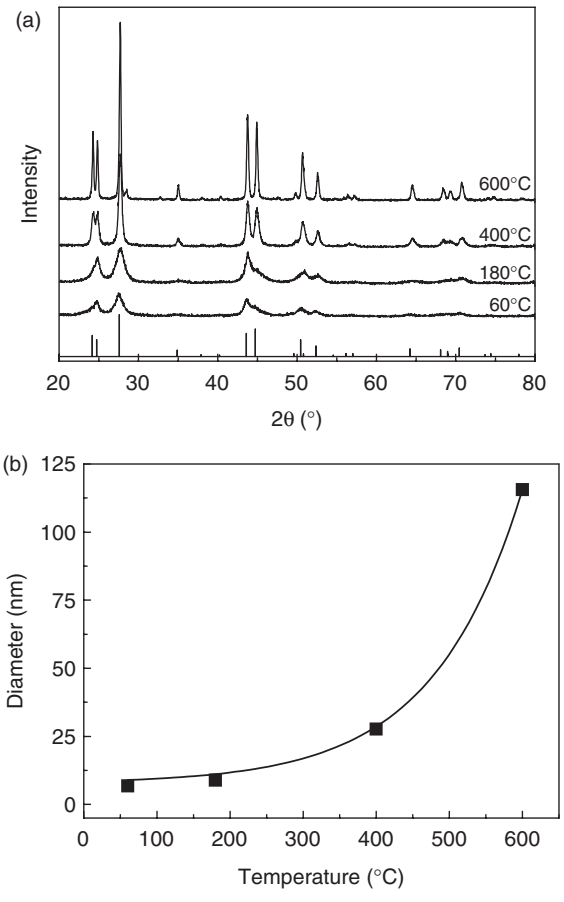

Figure 2. (a) XRD patterns of the 20 mol% Yb^{3+} and 2 mol% Er^{3+} co-doped LaF_3 nanoparticles synthesized at different temperatures. The line spectrum corresponds to the literature data of bulk LaF_3 (ICDD PDF No. 32-0483). (b) Dependence of the nanoparticle diameters estimated from the Scherrer equation on the temperatures.

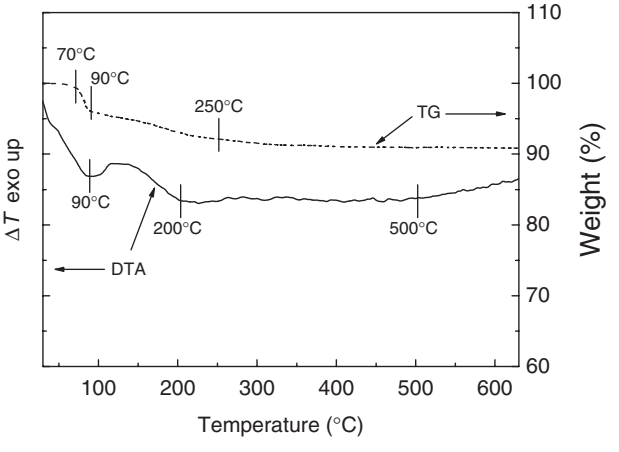

Figure 3. DTA (solid line) and TG (dash line) diagram of the as-prepared LaF_3:Yb^{3+},Er^{3+} nanoparticles.

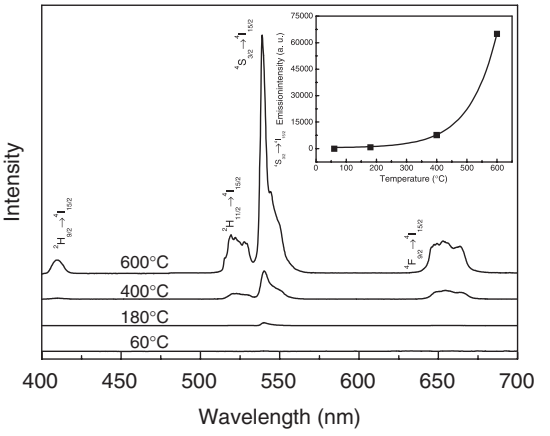

Figure 4. Upconversion emission spectra (excited with a 600 mW diode laser at 980 nm) of the 20 mol% Yb^{3+} and 2 mol% Er^{3+} co-doped LaF_3 nanoparticles synthesized at different temperatures. Inset: Relationship between the experimentally determined upconversion luminescence intensity on the synthesis temperature for the $^4S_{3/2} \rightarrow {}^4I_{15/2}$ emission of Er^{3+} from the LaF_3:Yb^{3+},Er^{3+} nanoparticles.

cross relaxation. On the other hand, the removal of OH^- groups from the particle surface and the increase of the particle size resulting from the heat treatment also reduced the loss of excited energy by surface defects. Therefore, the upconversion luminescence would be significantly strengthened with elevating heat treatment temperature. The inset of figure 4 shows the relationship between integrated green upconversion emission ($^4S_{3/2} \rightarrow {}^4I_{15/2}$) of Er^{3+} and the heat treatment temperature. The tendency of this curve exhibited a very good agreement with the curve shown in figure 2(b), implying the increase of the particles sizes is the major reason for the increase of the upconversion luminescence intensity.

Using the same method, 10 mol% Yb^{3+} ions and 2 mol% Tm^{3+} ions co-doped LaF_3 nanoparticles with blue upconversion emission were synthesized (heat treated at 60°C for 2 h). The upconversion spectrum of the nanoparticles is given in figure 5. The emission peaks at 450 nm, 476 nm, and 647 nm is ascribed to $^1D_2 \rightarrow {}^3F_4$, $^1G_4 \rightarrow {}^3H_6$ and $^1G_4 \rightarrow {}^3H_4$ transition of Tm^{3+}, respectively.

For the upconversion luminescence, the emission intensity and the power of laser resource present an exponential relationship. The logarithm of upconversion emission intensity depends linearly on the logarithm of excitation power and the slope of the beeline is the number of photons the excitation process required. Figure 6 gives the double logarithmic curves of upconversion emission intensities and excitation powers for LaF_3:Yb^{3+},Er^{3+} and LaF_3:Yb^{3+},Tm^{3+} nanoparticles. The slopes of the curves corresponding to the LaF_3:Yb^{3+},Er^{3+} upconversion emission at 411 nm and 539 nm were 2.65 and 1.83, which indicated that the two emissions were due to triple and double photons processes, respectively. The slope of the curve corresponding to the LaF_3:Yb^{3+},Tm^{3+} upconversion emission at 476 nm can be found to be 2.63, so the blue upconversion emission of Tm^{3+} was a triple photons process. This is in accordance with the upconversion mechanism of Er^{3+} and Tm^{3+} which was described by sequential two-photon absorption or energy transfer upconversion mechanisms [4, 19].

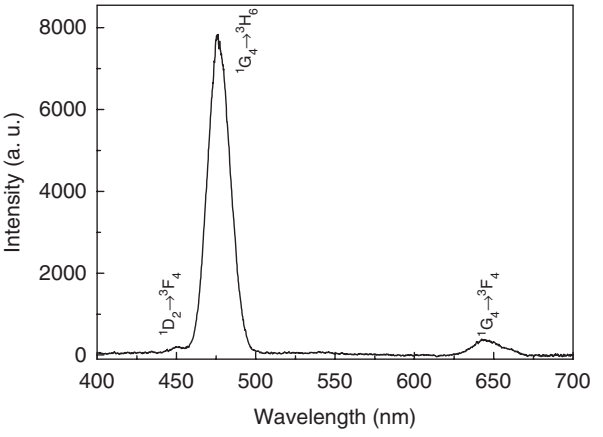

Figure 5. Upconversion emission spectrum (excited with a 600 mW diode laser at 980 nm) of the 10 mol% Yb^{3+} and 2 mol% Tm^{3+} co-doped LaF_3 nanoparticles synthesized at 600°C.

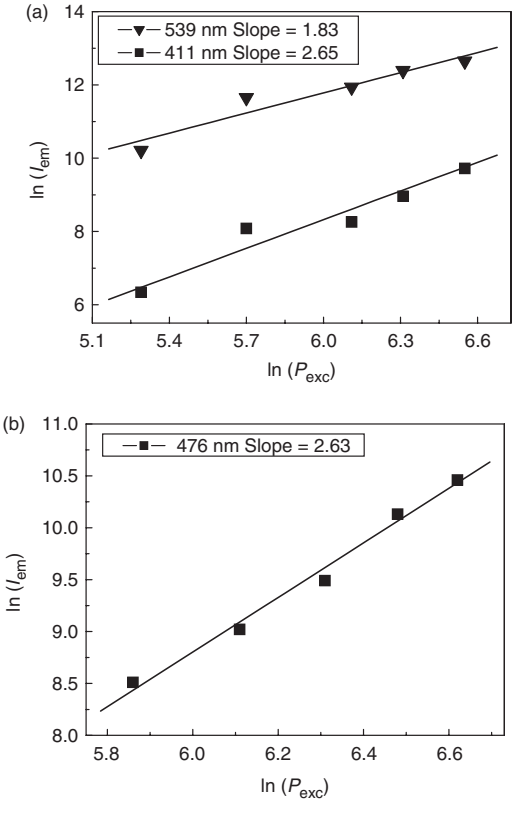

Figure 6. (a) Relationship between the upconversion luminescence intensity and the pumping power of diode laser for Er^{3+} 411 nm and 539 nm emissions from the 20 mol% Yb^{3+} and 2 mol% Er^{3+} co-doped LaF_3 nanoparticles. (b) Relationship between the upconversion luminescence intensity and the pumping power of diode laser for Tm^{3+} 476 nm emission from the 10 mol% Yb^{3+} and 2 mol% Tm^{3+} co-doped LaF_3 nanoparticles.

4. Conclusions

LaF_3:Yb^{3+},Ln^{3+} (Ln = Er, Tm) nanoparticles with upconversion luminescence were synthesized via a co-precipitation method, followed by heat treatment at 180°C, 400°C, and 600°C, respectively. The upconversion luminescence intensity of Yb^{3+}/Er^{3+} co-doped LaF_3 nanoparticles increased significantly, mainly due to the concurrent increase of the particle size, with increase of heat treatment temperatures. The samples consisted of well crystallized hexagonal phases. Their diameters remained in the nanometer scale at the heat treatment temperatures of 180°C and 400°C. The upconversion emissions of Er^{3+} at 411 nm and 539 nm were found to be triple and double photons processes, respectively. The 476 nm upconversion emission of Tm^{3+} can be ascribed to a triple photons process.

Acknowledgement

The authors gratefully acknowledge the support for this research from the National Nature Science Foundation of China (No.50472062) and Program for Changjiang Scholars and Innovative Research Team in University.

References

[1] E. Beaurepaire, V. Buissette, M.P. Sauviat, D. Giaume, K. Lahlil, A. Mercuri, D. Casanova, A. Huignard, J.L. Martin, T. Gacoin, J.P. Boilot, A. Alexandrou. Functionalized fluorescent oxide nanoparticles: Artificial toxins for sodium channel targeting and Imaging at the single-molecule level. *Nano Lett*, **4,** 2079 (2004).
[2] F. Meiser, C. Cortez, F. Caruso. Biofunctionalization of fluorescent rare-earth-doped lanthanum phosphate colloidal nanoparticles. *Angew. Chem.-Int. Edi*, **43,** 5954 (2004).
[3] F. Wang, W.B. Tan, Y. Zhang, X.P. Fan, M.Q. Wang. Luminescent nanomaterials for biological labelling. *Nanotechnology*, **17,** R1 (2006).
[4] F. Auzel. Upconversion and anti-stokes processes with f and d ions in solids. *Chemical Reviews*, **104,** 139 (2004).
[5] T. Soukka, K. Kuningas, T. Rantanen, V. Haaslahti, T. Lovgren. Photochemical characterization of up-converting inorganic lanthanide phosphors as potential labels. *J. Fluoresc*, **15,** 513 (2005).
[6] K. Konig. Multiphoton microscopy in life sciences, Part 2. *J. Microsc.-Oxf*, **200,** 83 (2000).
[7] K. Kuningas, T. Rantanen, T. Ukonaho, T. Lovgren, T. Soukka. Homogeneous assay technology based on upconverting phosphors. *Anal. Chem*, **77,** 7348 (2005).
[8] W. Denk, J.H. Strickler, W.W. Webb. 2-Photon Laser Scanning Fluorescence Microscopy. *Science*, **248,** 73 (1990).
[9] P.T.C. So, C.Y. Dong, B.R. Masters, K.M. Berland. Two-photon excitation fluorescence microscopy. *Annu. Rev. Biomed. Eng*, **2,** 399 (2000).
[10] S. Heer, O. Lehmann, M. Haase, H.U. Gudel. Blue, green, and red upconversion emission from lanthanide-doped $LuPO_4$ and $YbPO_4$ nanocrystals in a transparent colloidal solution. *Angew. Chem.-Int. Edit*, **42,** 3179 (2003).
[11] T. Hirai, T. Orikoshi Preparation of yttrium oxysulfide phosphor nanoparticles with infrared-to-green and -blue upconversion emission using an emulsion liquid membrane system. *J. Colloid Interface Sci*, **273,** 470 (2004).
[12] T. Hirai, T. Orikoshi, I. Komasawa. Preparation of Y_2O_3: Yb,Er infrared-to-visible conversion phosphor fine particles using an emulsion liquid membrane system. *Chemistry Of Materials*, **14,** 3576 (2002).
[13] G.S. Yi, B.Q. Sun, F.Z. Yang, D.P. Chen, Y.X. Zhou, J. Cheng. Synthesis and characterization of high-efficiency nanocrystal up-conversion phosphors: Ytterbium and erbium codoped lanthanum molybdate. *Chemistry Of Materials*, **14,** 2910 (2002).

[14] A. Aebischer, S. Heer, D. Biner, K. Kramer, M. Haase, H.U. Gudel. Visible light emission upon near-infrared excitation in a transparent solution of nanocrystalline beta-$NaGdF_4$: Yb^{3+}, Er^{3+}. *Chem. Phys. Lett*, **407,** 124 (2005).
[15] Y. Cui, X.P. Fan, Z.L. Hong, M.Q. Wang. Synthesis and luminescence properties of lanthanide (III)-doped YF_3 nanoparticles. *J. Nanosci. Nanotechnol*, **6,** 830 (2006).
[16] X.P. Fan, D.B. Pi, F. Wang, J.R. Qiu, M.Q. Wang. Hydrothermal synthesis and luminescence behavior of lanthanide-doped GdF_3 nanoparticles. *IEEE Trans. Nanotechnol*, **5,** 123 (2006).
[17] S. Heer, K. Kompe, H.U. Gudel, M. Haase. Highly efficient multicolour upconversion emission in transparent colloids of lanthanide-doped $NaYF_4$ nanocrystals. *Adv. Mater*, **16,** 2102 (2004).
[18] H.X. Mai, Y.W. Zhang, R. Si, Z.G. Yan, L.D. Sun, L.P. You, C.H. Yan. High-quality sodium rare-earth fluoride nanocrystals: Controlled synthesis and optical properties. *J. Am. Chem. Soc*, **128,** 6426 (2006).
[19] F. Wang, D.K. Chatterjee, Z.Q. Li, Y. Zhang, X.P. Fan, M.Q. Wang. One-pot synthesis of polyethylenimine/$NaYF_4$:Yb^{3+},Ln3$^+$ nanoparticles with up-conversion fluorescence. *Nanotechnology*, **17,** 5781 (2006).
[20] G.S. Yi, G.M. Chow. Colloidal LaF_3: Yb,Er, LaF_3: Yb,Ho and LaF_3: Yb,Tm nanocrystals with multicolor upconversion fluorescence. *J. Mater. Chem*, **15,** 4460 (2005).
[21] G.S. Yi, H.C. Lu, S.Y. Zhao, G. Yue, W.J. Yang, D.P. Chen, L.H. Guo. Synthesis, characterization, and biological application of size-controlled nanocrystalline $NaYF_4$: Yb,Er infrared-to-visible up-conversion phosphors. *Nano Lett*, **4,** 2191 (2004).
[22] J.H. Zeng, J. Su, Z.H. Li, R.X. Yan, Y.D. Li. Synthesis and upconversion luminescence of hexagonal-phase $NaYF_4$: Yb, Er^{3+}, phosphors of controlled size and morphology. *Adv. Mater*, **17,** 2119 (2005).
[23] G.J.H. De, W.P. Qin, J.S. Zhang, D. Zhao, J.S. Zhang. Bright-green upconversion emission of hexagonal LaF_3: Yb^{3+},Er^{3+} nanocrystals. *Chem. Lett*., **34,** 914 (2005).
[24] A. Kaminskii. *Laser Crystals, Their Physics and Properties*, Springer, New York (1990).
[25] O.V. Kudryavtseva, L.S. Garashina, K.K. Rivkina, B.P. Sobolev. Solubility of LnF_3 in lanthanum fluoride. *Sov. Phys. Crystallogr*., **18,** 531 (1974).
[26] J.W. Stouwdam, F. van Veggel. Near-infrared emission of redispersible Er^{3+}, Nd^{3+}, and Ho^{3+} doped LaF_3 nanoparticles. *Nano Lett*., **2,** 733 (2002).
[27] V. Sudarsan, F. van Veggel, R.A. Herring, M. Raudsepp. Surface Eu^{3+} ions are different than "bulk" Eu^{3+} ions in crystalline doped LaF_3 nanoparticles. *J. Mater. Chem*., **15,** 1332 (2005).
[28] F. Wang, Y. Zhang, X.P. Fan, M.Q. Wang. One-pot synthesis of chitosan/LaF_3:Eu^{3+} nanocrystals for bio-applications. *Nanotechnology*, **17,** 1527 (2006).
[29] F. Wang, Y. Zhang, X.P. Fan, M.Q. Wang. Facile synthesis of water-soluble LaF_3:Ln^{3+} nanocrystals. *J. Mater. Chem*, **16,** 1031 (2006).
[30] S.L. Zhao, Y.B. Hou, X.J. Pei, Z. Xu, X.R. Xu. Upconversion luminescence of $KZnF_3$:Er^{3+},Yb^{3+} synthesized by hydrothermal method. *J. Alloy. Compd*., **368,** 298 (2004).